From $[RuX_6]$ to $[Ru(RCN)_6]$: Synthesis of Mixed Halide–Nitrile Complexes of Ruthenium, and Their Spectroelectrochemical Characterization in Multiple Oxidation States

Colleen M. Duff[*,a] **and Graham A. Heath**[*,b]

[a] *Chemistry Department, University of New South Wales, Australian Defence Force Academy, Canberra, ACT 2600, Australia*

[b] *Research School of Chemistry, Australian National University, GPO Box 4, Canberra, ACT 2601, Australia*

A complete series of benzonitrile- and acetonitrile-substituted ruthenium halide complexes $[RuX_{6-n}(RCN)_n]^z$ (n = 0–6), ranging stepwise from $[RuX_6]^{2-}$ to $[Ru(RCN)_6]^{2+}$, has been prepared and characterized. Three series were established, having RCN/X = PhCN/Cl, PhCN/Br, and MeCN/Cl. The strategy of reductive substitution has been developed to prepare $[RuX_5(RCN)]^{2-}$, *trans*-$[RuX_4(RCN)_2]^-$, *mer*-$[RuX_3(RCN)_3]$ and *trans*-$[RuX_2(RCN)_4]$ in turn from $[RuX_6]^{2-}$ by systematic electrosynthetic routes, through detailed management of potential, temperature and RCN concentration. The monosubstituted pentahalogeno complexes are unstable and their preparation is only practicable *via* electrode-induced ($Ru^{IV} \longrightarrow Ru^{III}$) halide displacement from $[RuX_6]^{2-}$ at low temperature. At the divalent level, exhaustive substitution to form $[RuX(RCN)_5]^+$ and $[Ru(RCN)_6]^{2+}$ from $[RuX_2(RCN)_4]$ required more forcing chemical conditions (Ag^+ and CF_3SO_3H respectively). Voltammetric studies between −65 and 20 °C confirm that the family of mixed halide–nitrile monomeric complexes is rich in redox chemistry, spanning oxidation states V to II. Under reversible conditions, the various metal-based electrode potentials for $[RuX_{6-n}(RCN)_n]^z$ are a linear function of the stoichiometry parameter, n, increasing by 0.45 (Ru^V–Ru^{IV}) or 0.6 V (Ru^{IV}–Ru^{III} and Ru^{III}–Ru^{II}) per halide replaced by nitrile. By use of spectroelectrogeneration techniques, the optical charge-transfer spectra for every available member of each family have been recorded in multiple oxidation levels, defining the states Ru^{IV} for n = 0–2, Ru^{III} for n = 0–5 and Ru^{II} for n = 2–6. For the present complexes, there are unmistakable complementary progressions in the halide-to-metal ($X \rightarrow Ru^{III}$) and metal-to-ligand ($Ru^{II} \rightarrow RCN$) bands, in accord with the underlying trend in $E_{\frac{1}{2}}(Ru^{III}$–$Ru^{II})$. These measurements present an unusual opportunity to document and analyse the characteristic trends in appearance and location of both ligand-to-metal (Ru^{III}) and metal-to-ligand (Ru^{II}) charge-transfer manifolds as a function of stoichiometry.

Despite the vast descriptive chemistry of ruthenium, there is a generally acknowledged shortage of well defined, versatile, and convenient starting materials. One aspect of the present work was to demonstrate the value of the simple ruthenium(IV) hexahalide salts in this context, and to derive from them a range of successively nitrile-substituted complexes in lower oxidation states.

We have previously reported on reduction-induced halide substitution as a rational synthetic pathway to osmium(II) complexes,[1] and have now applied this technique to the electrochemical generation of a series of mixed halide–nitrile ruthenium complexes from the starting hexahalogenoruthenate(IV). Parallel work by Taylor and Yellowlees[2] has resulted in an analogous series of chloride–pyridine osmium complexes. The present paper covers the electrochemical and chemical syntheses for the entire series $[Ru_{6-n}(RCN)_n]^z$ (n = 0–6) where X = Cl, R = Me or Ph and X = Br, R = Ph. The earlier members of each series (n = 1–4) could be prepared electrochemically from $[RuX_6]^{2-}$ *via* reduction-induced spontaneous halide substitution. This has yielded thirteen halide–nitrile complexes by systematic routes.

For each stoichiometry there is also the possibility of generating alternative oxidation states, and these redox transformations have been exhaustively pursued by low-temperature electrolysis experiments. In this way, we have constructed extensive isovalent series $[RuX_{6-n}(RCN)_n]^z$, where n ranges from 0 to 3 for Ru^{IV}, from 0 to 5 for Ru^{III}, and from 2 to 6 for Ru^{II}. This includes seventeen otherwise inaccessible species and appears to represent the practical limits of stability for the present systems.

The availability of such complete series, MX_6 to ML_6, is of interest in its own right, particularly given the periodic patterns in electrode potentials established for the 4d and 5d transition-metal hexahalides.[3] If similar periodic patterns exist for specifically substituted complexes, such as MX_4L_2 (only M varying), then the corollary is that for a given metal there must be a systematic change in redox potential in the complexes $MX_{6-n}L_n$ as a function of stoichiometry (only n varying).

Systematic trends in metal-based electrode potentials with the degree of halide ligation have been one of the fundamental concerns in this laboratory. In addition we seek an overall picture of the structure and location of halide-to-metal charge-transfer absorption bands in substituted complexes of the form $MX_{6-n}L_n$. Moreover, there should be a rational relationship between optical charge-transfer processes and the redox behaviour of the metal centre in such co-ordination complexes. The mixed halide–nitrile complexes presented here provide an excellent opportunity for exploring these three questions in a coherent way. In the present paper we describe fully the electrochemical and chemical syntheses of each series and the

detailed appearance of the charge-transfer spectra. The trends in metal-based electrode potentials and charge-transfer band energies for the series $[RuX_{6-n}(RCN)_n]^z$ are discussed elsewhere.[4]

Experimental

Cyclic voltammetric measurements (typically $v = 100$ mV s^{-1}) were made with either a PAR 170 or BAS 100 electrochemistry system. Phase-sensitive alternating current (a.c.) measurements ($\omega = 205$ Hz, $v = 10$ mV s^{-1}) were made with the PAR 170 system. The electrolyte, NBu_4BF_4, was prepared by neutralizing NBu_4OH (40% in water) with HBF_4 to pH 5. The precipitate was filtered and recrystallized twice from methanol–water then twice from ethyl acetate–diethyl ether and dried *in vacuo* at 100 °C for 8 h. The final recrystallization was repeated until a sufficient electrochemical background was achieved. Electrochemical solutions were 0.5 mol dm^{-3} NBu_4BF_4 in CH_2Cl_2 (or mixed CH_2Cl_2–nitrile solvents) or 0.1 mol dm^{-3} NBu_4BF_4 in nitrile solvents and approximately 10^{-3} mol dm^{-3} in sample. All solutions were purged and maintained under an atmosphere of N_2, except when ruthenium(II) species were generated, in which case Ar was used. A jacketted glass cell (5 cm^3) was used with a platinum working micro-electrode (0.5 mm), a platinum-wire counter electrode, and a non-aqueous Ag–AgCl reference electrode. Low temperatures were achieved with a Lauda model RL6 circulating cryostat bath. The preparation of the reference electrode has been reported elsewhere.[4] The ferrocenium–ferrocene couple appeared at +0.564 V under these conditions at room temperature, in CH_2Cl_2.

Electronic spectra (45 000–5000 cm^{-1}) were directly recorded linear in frequency on a Perkin-Elmer Lambda 9 spectrophotometer. Spectra of complexes in alternative oxidation states were obtained by electrogeneration within a cryostatted optically transparent electrochemical cell (pathlength 0.5 mm) mounted within the spectrometer.[4] Charge-transfer spectra of $[RuX_5(RCN)]^{2-}$, $[RuX_5(RCN)]^-$, $[RuBr_3(PhCN)_3]$ and $[RuCl_2(MeCN)_4]$ were collected by electrosynthesis from precursors of different stoichiometry in the above cell as described below. Infrared spectra were collected on a Perkin-Elmer 1600 spectrometer. Samples were prepared as KCl or KBr discs (3300–600 cm^{-1}) or polyethylene discs (600–150 cm^{-1}). Proton and ^{13}C NMR spectra were obtained with a Bruker WM 300 MHz spectrometer at both ambient temperature and at −70 °C in CD_2Cl_2 or $CDCl_3$ and were referenced to $SiMe_4$ at 0 ppm.

Elemental analyses were performed by the Micro-analytical Laboratory, Research School of Chemistry, Australian National University.

All solvents were analytical grade and distilled under N_2 from the appropriate drying agent prior to use. Pure $[NBu_4]_2[RuCl_6]$ was prepared by treatment of $[RuCl_6]^{3-}$ with Cl_2 in hydrochloric acid solution followed by addition of NBu_4Cl.[5] The salt $[NBu_4]_2[RuBr_6]$ was prepared as reported by Preetz and Allworden[6] and $K_3[Ru_2Br_9]$ according to Fergusson and Greenaway;[7] $K_3[RuCl_6]$ was purchased from Aldrich Chemical Company and $RuCl_3 \cdot xH_2O$ from J.J. Matheson Company. Triflic acid (CF_3SO_3H) was purchased from Aldrich and distilled under reduced pressure prior to use. Analytical data for all compounds appear in Table 1.

Non-electrochemical Synthesis.—$[NBu_4][RuCl_4(PhCN)_2]$. A solution of $[NBu_4]_2[RuCl_6]$ (0.54 g, 0.68 mmol) in PhCN (25 cm^3) was heated to reflux for *ca.* 20 h. The orange-yellow product precipitated after the addition of diethyl ether and was recrystallized twice from CH_2Cl_2 and diethyl ether to give 0.34 g of orange needle-shaped crystals (72%). The salt $[NBu_4][RuCl_4(MeCN)_2]$ was prepared by an analogous method, typically yielding 65–70% of yellow product.

$[RuCl_3(MeCN)_3]$. The salt $[NBu_4][RuCl_4(MeCN)_2]$ (0.20 g, 0.352 mmol) was stirred with $NaBF_4$ (0.06 g, 0.546 mmol) in MeCN (10 cm^3) under reflux for 1 h. After cooling, the precipitated NaCl was removed by filtration through Celite and the crude product isolated by complete removal of solvent at reduced pressure. The solid was recrystallized from MeCN and diethyl ether and further purified by flash chromatography. The product, dissolved in MeCN, was loaded on a 10 cm × 2 cm column of dried Kiesel gel 60 and eluted with MeCN–CH_2Cl_2 (30:70). The major fraction was collected and recrystallized from MeCN–diethyl ether to give 0.06 g (52% yield).

$[RuCl_3(PhCN)_3]$. This was prepared by a modification of the synthesis reported by Dehand and Rose.[8] Ruthenium trichloride hydrate (1.23 g, 4.7 mmol) was heated to 80 °C in a mixture of methanol (5 cm^3) and PhCN (20 cm^3) for 45 min. Diethyl ether was added to the resulting deep red solution to isolate the product. Precipitation from PhCN–CH_2Cl_2 (10:90) with diethyl ether yielded 2.12 g (82% yield).

$[RuCl_2(RCN)_4]$ (R = Ph *or* *p*-MeC_6H_4). This procedure is identical to that for $[RuCl_3(PhCN)_3]$ with the exception of the reaction temperature and time. Following mild heating (80 °C) for 4 h the mixture was heated to 120 °C for 48 h. Completion of the reaction was easily identified by the stark change in colour from deep red orange to yellow. The product was largely insoluble and the precipitated portion was collected. Addition of diethyl ether to the supernatant precipitated a second fraction. The purity of the yellow powder was sufficient without further recrystallization (average yield: R = Ph, 89; *p*-tolyl, 91%).

$[RuCl_2(p\text{-}MeC_6H_4CN)_4]$: δ_H(300 MHz, CD_2Cl_2) 2.45 (s), 7.33 (d) and 7.73 (d, $J = 123$ Hz); δ_C(300 MHz, CD_2Cl_2) 21.4 (Me), 108.9 (ipso), 123.6 (CN), 129.5 (*para*), 132.8 (*meta*) and 144.0 (*ortho*).

$[RuCl(PhCN)_5]BF_4$. Treatment of $[RuCl_2(PhCN)_4]$ (0.36 g, 0.62 mmol) with $AgBF_4$ (0.14 g, 0.72 mmol) in PhCN at 100 °C for 2 h yielded the required complex. Filtration through Celite was followed by addition of diethyl ether–pentane (50:50) to initiate precipitation. Recrystallization from a 5% mixture of PhCN in CH_2Cl_2 and diethyl ether gave 0.42 g yellow powder (91% yield). The salt $[RuBr(PhCN)_5]BF_4$ was prepared by an analogous method typically yielding 85–90% of orange-yellow product.

$[NBu_4][RuBr_4(PhCN)_2]$. A solution of $K_3[Ru_2Br_9]$ (0.50 g, 0.53 mmol) and NBu_4Br (0.35 g, 1.1 mmol) in PhCN (10 cm^3) was stirred at ambient temperature for 16 h. The resultant deep purple mixture was filtered through Celite to remove KBr, and diethyl ether–pentane (50:50) was added to precipitate the product. The purple powder was recrystallized twice from a mixture of CH_2Cl_2–diethyl ether to give 0.59 g (74% yield).

$[RuBr_2(PhCN)_4]$. A solution of $[NBu_4][RuBr_4(PhCN)_2]$ (0.39 g, 0.53 mmol) in a mixture of methanol (15 cm^3) and PhCN (10 cm^3) was heated to 120 °C for 48 h. On cooling the deep yellow product precipitated and was collected by filtration. Its purity was sufficient without recrystallization; 0.29 g was isolated (79% yield).

$[Ru(PhCN)_6][CF_3SO_3]_2$. Under strictly dry anaerobic conditions, $[RuCl(PhCN)_5]BF_4$ (0.31 g, 0.42 mmol) was heated in triflic acid (15 cm^3) at 100 °C for 1.5 h. After cooling, diethyl ether (25 cm^3) was added to dilute the acid, followed by PhCN (5 cm^3). The reaction mixture was added to water, the organic phase separated, washed with water, and dried over anhydrous Na_2SO_4. Reduction of the volume followed by the addition of pentane yielded 0.34 g of a very pale yellow solid (80% yield).

Electrochemical Synthesis.—Electrolytic experiments were performed with either a PAR 170 or PAR 174A potentiostat. A three-compartment H-cell was used with a platinum-mesh basket as working electrode, a non-aqueous Ag–AgCl reference, a platinum micro-electrode to monitor the electrolysis and a platinum coil as counter electrode separated from the working compartment by a salt bridge. Electrolyte solutions were prepared and purged as those used in voltammetry. Isolable electrogenerated complexes either precipitated from solution or were separated from the electrolyte by washing with benzene to remove the major fraction of NBu_4BF_4, followed by repeated

Table 1 Analytical data (%) with calculated values in parentheses

Complex	C	H	N	X
$[NBu_4]_2[RuCl_6]$	47.90 (48.10)	9.55 (9.10)	3.45 (3.50)	26.40 (26.65)
$[NBu_4]_2[RuBr_6]$	36.40 (36.05)	7.15 (6.80)	2.60 (2.65)	45.00 (45.00)
$[NBu_4][RuCl_4(PhCN)_2]$	51.80 (52.10)	6.60 (6.70)	5.95 (6.10)	19.80 (20.50)
$[NBu_4][RuCl_4(MeCN)_2]$	41.80 (42.35)	7.55 (7.45)	7.05 (7.40)	24.85 (25.00)
$[NBu_4][RuBr_4(PhCN)_2]$	41.45 (40.95)	5.35 (5.50)	4.85 (4.75)	36.75 (36.85)
$[RuCl_3(PhCN)_3]$*	49.70 (50.15)	3.00 (2.95)	8.25 (8.25)	20.00 (20.25)
$[RuCl_3(MeCN)_3]$	21.70 (21.80)	2.65 (2.75)	12.25 (12.70)	32.15 (32.15)
$[RuCl_2(p\text{-}MeC_6H_4CN)_4]$	59.85 (60.00)	4.60 (4.40)	8.85 (8.75)	11.25 (11.05)
$[RuCl_2(PhCN)_4]$	57.55 (57.25)	3.45 (3.80)	9.60 (9.85)	12.15 (11.75)
$[RuBr_2(PhCN)_4]$	49.70 (49.95)	2.80 (3.00)	8.30 (8.30)	24.30 (23.75)
$[RuCl(PhCN)_5]BF_4$	56.90 (57.05)	3.40 (3.55)	9.50 (9.70)	4.80 (4.70)
$[RuBr(PhCN)_5]BF_4$	53.65 (54.00)	3.20 (3.35)	8.95 (9.00)	10.20 (10.15)
$[Ru(PhCN)_6][CF_3SO_3]_2$	51.90 (51.55)	2.95 (2.90)	8.25 (8.00)	11.20 (10.10)

* Calculated for ·0.14 PhCN solvate.

Table 2 Electrochemical data for $[RuX_{6-n}(RCN)_n]^{z/z-}$ measured under the conditions indicated[a]

X = Cl⁻, L = PhCN				X = Cl⁻, L = MeCN				X = Br⁻, L = PhCN		
n	V–IV	IV–III	III–II	*n*	V–IV	IV–III	III–II	*n*	IV–III	III–II
0[b]	1.78	0.22	−1.51	0[b]	1.78	0.22	−1.51	0[b]	0.14	−1.46[d]
1[c]	2.23	0.86	−0.80[d]	1[c]	2.20	0.82	—	1[e]	0.78	—
2[b]		1.45	−0.27	2[b]	—	1.45	−0.38	2[b]	1.41	−0.15
3[e]		2.03	0.39	3[e]	—	1.89	0.29	3[e]	—	0.38
4		—	1.02[b]	4	—	—	0.84[e]	4[b]	—	0.97
5[f]		—	1.60					5[f]	—	1.55
6[f]		—	2.23					6[f]	—	2.23

[a] Statistical survey suggests that comparable reversible couples are *ca.* 65 mV more negative than values determined in MeCN and expressed *vs.* normal hydrogen electrode (NHE). [b] In CH_2Cl_2 at −70 °C. [c] In 10% RCN–CH_2Cl_2 at −30 °C. [d] $E_{\frac{1}{2}}$ was estimated from the cathodic peak. [e] In 20% RCN–CH_2Cl_2 at −30 °C. [f] In CH_2Cl_2 at room temperature.

crystallization from an appropriate solvent. Electrolyses were continued to *ca.* 99% completion (based on current passing), and until voltammetric analysis of the product solutions indicated quantitative conversions. Yields of isolated, pure products (X = Cl or Br; RCN = MeCN or PhCN) varied from 20 to 70% depending on the work-up procedure and the scale of the synthesis.

$[RuX_5(RCN)]^{-/2-}$. Electrochemical reduction of $[NBu_4]_2[RuX_6]$ to Ru^{III} in 10% nitrile–CH_2Cl_2 at −0.1 V and −30 °C (−60 °C in 50% RCN–CH_2Cl_2) generated $[RuX_5(RCN)]^{2-}$. In order to stabilize $[RuX_5(RCN)]^{2-}$ from further substitution it was oxidized back to Ru^{IV} at 0.7 V at low temperature (−50 °C). Attempts to isolate this complex in either the ruthenium-(IV) or -(III) states were unsuccessful. Cannula transfer of $[RuX_5(RCN)]^-$ to dry Et_2O at low temperature caused the precipitation of a mixture of $[RuX_4(RCN)_2]^-$ and $[RuX_6]^{2-}$. Similar treatment of $[RuX_5(RCN)]^{2-}$ yielded mainly $[RuX_4(RCN)_2]^-$.

$[RuX_4(RCN)_2]^-$. When the preceding electrogeneration was performed and then allowed to warm to room temperature a second halide was substituted by nitrile producing $[RuX_4(RCN)_2]^-$. This complex was stable to further substitution at the ruthenium(III) level and could be characterized *in situ*, or isolated from the electrochemical medium by repeated fractional crystallization from CH_2Cl_2–Et_2O.

$[RuX_3(RCN)_3]$. Reduction of $[RuX_4(RCN)_2]^-$ to Ru^{II} at −0.5 V in 10% RCN–CH_2Cl_2 at −30 °C (−55 °C in 70% RCN) cleanly yielded $[RuX_3(RCN)_3]^-$. The ruthenium(II) complex undergoes further substitution at higher temperatures and in order to stabilize this stoichiometry it was oxidized to Ru^{III} at +0.5 V and −50 °C. The complex is stable at the ruthenium(III) level and could be isolated at ambient temperature. Separation from the electrolyte was achieved by flash chromatography as outlined in the chemical synthesis above.

$[RuX_2(RCN)_4]$. When electrogenerated as above, $[RuX_3(RCN)_3]^-$ underwent further substitution at room temperature in 10% RCN–CH_2Cl_2 to give $[RuX_2(RCN)_4]$, which precipitated from the electrochemical medium and was collected by filtration.

Results

Voltammetry and Electrosynthesis.—The voltammetric response of each complex of the series $[RuX_{6-n}(RCN)_n]^z$ was determined in both a non-co-ordinating medium (CH_2Cl_2) and in the appropriate nitrile solvent at a variety of temperatures. The complexes $[RuX_6]^{2-}$, $[RuX_5(RCN)]^-$, $[RuX_4(RCN)_2]^-$ and $[RuX_3(RCN)_3]$ were found to undergo ligand substitution upon reduction in co-ordinating solvents and this tendency was investigated as a function of temperature and concentration of nitrile. Electrode potentials for accessible reductions and/or oxidations, measured under reversible conditions, are listed in Table 2. For each of the tabulated voltammetric experiments the conditions were chosen to achieve reversibility. In other words, coupled chemical reactions were eliminated by control of temperature and nucleophile concentration. Separation of the anodic (E_a) and cathodic (E_c) peaks of the cyclic voltammogram, and the width at half height of the a.c. peak, as compared to internal ferrocene, were the criteria used in assessing reversibility. The $E_{\frac{1}{2}}$ values in Table 2 were obtained from a.c. voltammetry and were compared to the ferrocenium–ferrocene couple of added ferrocene when this did not interfere with the couple of interest. In addition, all couples were checked against either $E_{\frac{1}{2}}(Ru^{IV}–Ru^{III})$ of added $[NBu_4]_2[RuX_6]$ or $E_{\frac{1}{2}}(Ru^{III}–Ru^{II})$ of added $[NBu_4][RuX_4(RCN)_2]$ for internal consistency.

The three accessible electrode potentials ($Ru^{V}–Ru^{IV}$, $Ru^{IV}–Ru^{III}$, $Ru^{III}–Ru^{II}$) exhibit a general trend to more positive values across each series, RuX_6 to RuL_6.

Electrosynthesis.—The conditions under which reduction

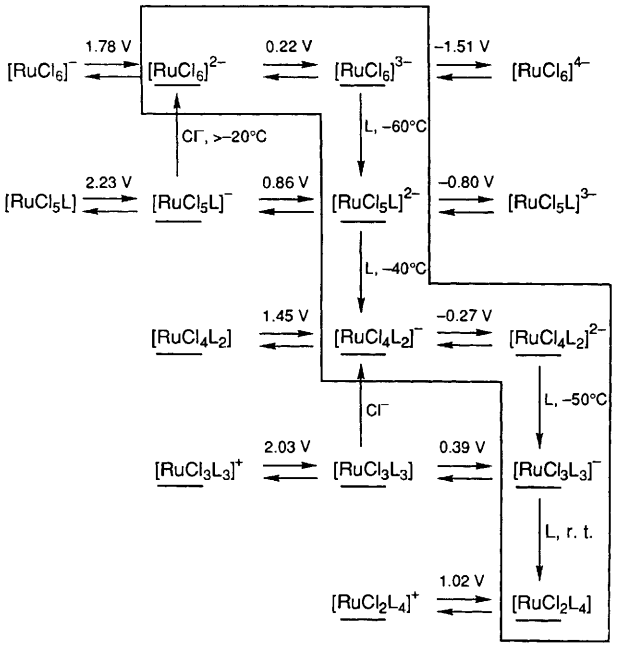

Scheme 1 Electrochemical scheme showing all voltammetrically detected species and the pathways between them. Underlined complexes were generated in bulk electrolytic experiments. The highlighted pathway shows the stepwise electrosynthetic route from $[RuCl_6]^{2-}$ to $[RuCl_2(PhCN)_4]$ *via* controlled reduction-induced halide substitution. General conditions are given, see Experimental section for greater detail; r.t. = room temperature

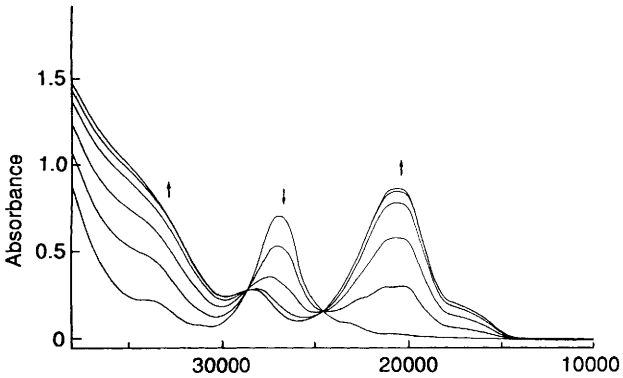

Fig. 1 Spectroelectrogeneration of $[Ru^{IV}Cl_5(MeCN)]^-$ from $[RuCl_5(MeCN)]^{2-}$ at −65 °C in 5% MeCN–CH_2Cl_2. The solution was 0.5 mol dm^{-3} in NBu_4BF_4 and *ca.* 10^{-3} mol dm^{-3} in $[RuCl_5(MeCN)]^{2-}$. The $[RuCl_5(MeCN)]^{2-}$ was electrochemically generated *in situ* from $[NBu_4]_2[RuCl_6]$ at 50 °C and 0.0 V prior to the spectroelectrogeneration

was linked to halide displacement, as determined by voltammetry, were transferred to bulk electrolysis to generate quantitatively a new stoichiometry. Electrochemical routes from $[RuCl_6]^{2-}$ to $[RuCl_2(RCN)_4]$ are shown in Scheme 1. The highlighted pathway shows the irreversible processes involving changes *in both* stoichiometry and oxidation state.

Charge-transfer Spectra.—The underlined complexes in any horizontal line of Scheme 1 represent compounds generated by change in oxidation state with no change in stoichiometry. These reversible electrolysis experiments were performed within the spectrophotometer compartment in a cryostatted thin-layer (pathlength 0.5 mm) electrochemical cell. This technique allowed the collection of charge-transfer spectra for each compound in all accessible oxidation states. Thus, the spectroscopic data available from the basis set of twelve complexes were extended to include an additional four non-isolated, unstable species $[RuX_5(RCN)]$ (R = Me or Ph, X = Cl or Br) and $[RuBr_3(PhCN)_3]$, and a further seventeen complexes in alternate oxidation states.

Precise isosbestic points in the sequential spectra collected during *in situ* electrogeneration are consistent with the presence of a single electrode product in each case. If an equilibrium involving the electrogenerated species were to be instantaneously established, isosbestic points would also be observed, however this possibility is eliminated by the exact reproduction of results at different temperatures and different concentrations. Fig. 1 shows the reversible oxidation of $[RuCl_5(MeCN)]^{2-}$ in 0.5 mol dm^{-3} NBu_4BF_4–5%MeCN–CH_2Cl_2 at −65 °C. Upon completion, full chemical reversibility was demonstrated by reversing the electrochemical process to recover the original spectrum intact. These criteria of chemical reversibility during spectroelectrogeneration have been applied in each case. The spectral data for the compounds as isolated and for their electrogenerated alternative oxidation states are listed in Table 3. The charge-transfer bands (X p_π ⟶ Ru^{III} t_{2g} and Ru^{II} t_{2g} ⟶ RCN p_π^*) for the various systems are shown in Figs. 2 (Ru^{II}–Cl–PhCN), 3 (Ru^{III}–Cl–PhCN) and 4 (Ru^{III}–Br–PhCN).

Discussion

Reduction-induced halide substitution in the electrochemical synthetic route yielded $[RuX_2(RCN)_4]$ as the lowest halide-containing stoichiometry at Ru^{II} and the preparation of $[RuX(RCN)_5]^+$ and $[Ru(RCN)_6]^{2+}$ required chemical methods. Silver ion adequately removes one halide from $[RuX_2(RCN)_4]$, however a more rigorous halide-abstracting agent was required to remove the final halide from $[RuX(RCN)_5]^+$. Hot concentrated triflic acid was found to be sufficient, but was only successful under strictly anaerobic conditions. It is assumed that the intermediate in this reaction is $[Ru(PhCN)_{6-n}(CF_3SO_3)_n]$ but no attempts were made to isolate such species. Concentrated triflic acid has been reported to polymerize benzonitrile, however co-ordinated benzonitrile is robust under these conditions and the additional benzonitrile necessary for the substitution reaction was added following dilution of the reaction mixture with dry ether to prevent polymerization. The complex $[Ru(MeCN)_6][p\text{-}MeC_6H_4SO_3]_2$ has been previously prepared from $[Ru(H_2O)_6]^{2+}$ and the crystal structure solved.[9,10] The preparation of $[Ru(H_2O)_6]^{2+}$ is difficult and the current synthesis is equally reliable and consists of two steps from $RuCl_3{\cdot}xH_2O$. The Ru^{III}–Ru^{II} electrode potential for the hexakis(nitrile) complex has not been previously detected.[10] Its appearance at 2 V more positive than the same couple for $[Ru(NH_3)_6]^{2+}$ was perhaps not anticipated by the previous authors.

The *trans* isomers of $[RuX_4L_2]^-$ and RuX_2L_4, and the *meridional* isomer of $[RuX_3(RCN)_3]$, were isolated. Spectroscopic and electrolytic experiments were carried out in both non-co-ordinating media and in nitrile solvents, and at no time was there any indication of isomerization. The *trans* geometries are suggested by the single ν_{CN} bands in the infrared spectra of $[RuCl_2(PhCN)_4]$ (2244s cm^{-1}) and $[RuCl_4(PhCN)_2]^-$ (2267vw cm^{-1}), and the *meridional* geometry by three ν_{CN} bands for $[RuCl_3(PhCN)_3]$ (2265s, 2253(sh) and 2230m cm^{-1}). These assignments are also consistent with the general appearance of the associated ruthenium(III) charge-transfer manifolds, which are characteristic of stoichiometry and structure (see below). The assigned structures have been verified by X-ray structural analysis for *trans*-$[NBu_4][RuCl_4(PhCN)_2]$ and *mer*-$[RuCl_3(PhCN)_3]$,[11] and by the highly symmetric ^1H and ^{13}C NMR spectra of *trans*-$[RuCl_2(p\text{-}MeC_6H_4CN)_4]$ (NMR data are included in the Experimental section). The tolyl nitrile derivative was examined since *trans*-$[RuCl_2(RCN)_4]$ (R = Me or Ph) are only sparingly soluble. The benzonitrile and tolyl nitrile

Table 3 Spectral data for $[RuX_{6-n}(RCN)_n]^z$, collected in CH_2Cl_2 at room temperature unless otherwise noted. Band maxima are given in cm^{-1} and molar absorptivity in $dm^3\ mol^{-1}\ cm^{-1}$ (in parentheses)

Ru^{IV}										
$[RuCl_5(PhCN)]^-$ *	16 200 (4 140)	17 400 (4 630)	20 500 (7 960)	24 200 (sh)		$[RuCl_4(MeCN)_2]$ *	17 800 (4 300)	19 600 (3 900)	25 200 (1 100)	27 400 (1 300)	39 900 (9 800)
$[RuCl_5(MeCN)]^-$ *	16 500 (1 650)	17 500 (2 040)	20 600 (6 430)	28 400 (2 570)		$[RuCl_4(PhCN)_2]$ *	17 910 (6 800)	19 140 (6 900)	27 400 (1 700)	35 600 (9 400)	
$[RuBr_5(PhCN)]^-$ *	12 000 (1 200)	13 600 (3 200)	15 100 (4 900)	16 250 (4 500)		$[RuCl_3(MeCN)_3]^+$ *	15 000 (840)	22 250 (5 500)	3 080 (1 000)	39 000 (sh)	
Ru^{III}										
$[RuCl_5(PhCN)]^{2-}$ *	20 500 (2 540)	22 500 (3 070)	26 400 (8 410)	29 800 (9 070)	32 200 (6 580)	$[RuCl_3(MeCN)_3]$	20 850 (820)	24 800 (3 800)	34 500 (1 100)	38 800 (1 400)	
$[RuCl_5(MeCN)]^{2-}$ *	23 400 (1 020)	27 000 (5 246)	34 000 (2 040)			$[RuBr_3(PhCN)_3]$	14 800 (790)	18 000 (3 200)	27 300 (5 600)	34 000 (10 900)	
$[RuBr_5(PhCN)]^{2-}$ *	16 900 (sh)	17 900 (800)	19 750 (1 200)	21 400 (3 400)	29 350 (4 100)	31 000 (10 200)	$[RuCl_2(PhCN)_4]^+$ *	21 460 (5 000)	32 510 (6 200)		
$[RuCl_4(PhCN)_2]^-$	20 510 (550)	23 720 (6 060)	24 500 (6 000)	32 200 (12 500)		$[RuCl_2(p\text{-}MeC_6H_4CN)_4]^+$ *	21 300 (8 900)	32 900 (11 000)			
$[RuCl_4(MeCN)_2]^-$	21 150 (510)	24 250 (5 900)	25 200 (5 400)	32 810 (2 100)	40 000 (8 100)	$[RuBr_2(PhCN)_4]^+$ *	15 700 (8 400)	19 800 (1 300)	24 300 (1 300)		
$[RuBr_4(PhCN)_2]^-$	14 900 (470)	17 500 (5 000)	19 600 (4 800)	31 600 (16 000)		$[RuCl(PhCN)_5]^{2+}$ *	19 100 (10 000)				
$[RuCl_3(PhCN)_3]$	20 000 (740)	23 787 (4 100)	35 490 (20 000)	36 180 (20 000)							
Ru^{II}											
$[RuCl_4(PhCN)_2]^{2-}$ *	23 063 (17 000)	$[RuBr_3(PhCN)_3]^-$ *	26 100 (17 000)			$[RuCl(PhCN)_5]^+$	33 200 (46 000)				
$[RuBr_4(PhCN)_2]^{2-}$ *	22 600 (14 000)	$[RuCl_2(PhCN)_4]$	29 270 (18 000)			$[RuBr(PhCN)_5]^+$	33 300 (44 000)				
$[RuCl_3(PhCN)_3]^-$ *	25 693 (15 000)	$[RuCl_2(p\text{-}MeC_6H_4CN)_4]$	28 640 (20 000)	31 220 (31 000)		$[Ru(PhCN)_6]^{2+}$	36 230 (58 000)				
$[RuCl_3(MeCN)_3]^-$ *	41 800 (12 200)	$[RuBr_2(PhCN)_4]$	28 440 (15 000)	30 500 (23 000)							

* Spectrum obtained by *in situ* electrogeneration as described in the text.

analogues may be taken to share the same geometry since they have virtually identical infrared and charge-transfer spectra at both ruthenium-(II) and -(III) levels (see Table 3).

Voltammetry and Electrosynthesis.—In preparative coordination chemistry electrochemical methods lend themselves naturally to situations where a change in oxidation state is the prime objective. Electrolysis has not been as widely exploited when the aim is to alter the composition of a complex by ligand substitution, despite the familiarity of situations where halide displacement is linked to chemical reduction of the metal centre. We have found that electrochemical reduction of the metal centre effectuates the substitution of halide by nitrile ligands, and through the control of temperature and nucleophile concentration impressive synthetic routes have resulted. The strategy of this work has been first to explore by voltammetry the reduction-induced substitution reactions as a function of temperature and neutral ligand concentration, and then to extend these conditions to bulk electrolysis.

This is illustrated by the electrochemical response of $[RuCl_6]^{2-}$ in a mixed MeCN–CH_2Cl_2 solvent system. Fig. 5 shows the cyclic voltammetry of $[RuCl_6]^{2-}$ in 5% MeCN–CH_2Cl_2 at both −60 °C [Fig. 5(*a*)] and room temperature [Fig. 5(*b*)] in the range of 0.0–2.0 V *vs.* Ag–AgCl. At low temperature the voltammogram exhibits a reversible Ru^V–Ru^{IV} oxidation at +1.78 V and a reversible Ru^{IV}–Ru^{III} reduction at +0.22 V. At room temperature the reduction at 0.22 V becomes completely irreversible. The cathodic peak appearing at +0.15 V is nearly unshifted, but the return anodic peak is completely absent. The new, reversible Ru^{IV}–Ru^{III} couple at +0.82 V is due to the substituted species $[RuCl_5(MeCN)]^{2-}$ which is generated at the electrode surface as $[RuCl_6]^{2-}$ is reduced [Fig. 5(*b*)]. Thus the hexahalide is stable to halide displacement in the ruthenium(IV) oxidation state, but substitution occurs readily upon reduction to Ru^{III}.

The reduction-induced halide-displacement reactions can also be controlled by altering the temperature and the concentration of incoming ligand. For example, in 5% MeCN–CH_2Cl_2 at −60 °C, the Ru^{IV}–Ru^{III} couple of $[RuCl_6]^{2-}$ behaves reversibly, while in 50% MeCN–CH_2Cl_2 at −60 °C chloride is replaced by nitrile upon reduction to give $[RuCl_5(MeCN)]^{2-}$.

Extension of these voltammetric observations led to an electrolytic experiment that efficiently yielded $[RuCl_5(MeCN)]^{2-}$ in bulk solution. The complex $[RuCl_5(PhCN)]^-$ has been claimed,[12] however the reported absorption spectrum is inconsistent with our results. Attempts to repeat the literature synthesis resulted in mixtures with $[RuCl_4(PhCN)_2]^-$ as the major identifiable fraction. Alternate synthetic routes were equally unsuccessful and electrosynthesis proved to be the only route to this stoichiometry. Heating $[NBu_4]_2[RuCl_6]$ in nitrile produced the disubstituted product $[RuCl_4(RCN)_2]^-$. This reaction was monitored by ultraviolet–visible spectroscopy and at no point was a monosubstituted complex $[RuCl_5(RCN)]^z$ detected. This is consistent with the observed instability of the pentahalide complexes when electrogenerated. The complexes $[RuCl_5(PhCN)]^{2-}$, $[RuCl_5(MeCN)]^{2-}$, $[RuBr_5(PhCN)]^{2-}$ and $[RuBr_5(MeCN)]^{2-}$ were electrogenerated by the reduction of $[RuX_6]^{2-}$ in the presence of RCN (Scheme 1) and each could be reoxidized *in situ* to the corresponding ruthenium(IV) monoanion. These transformations were only possible at low temperature and with strict regard to the applied potential. On warming to room temperature the bromide complexes underwent further substitution at both the ruthenium-(III) and -(IV) states. The chloride complexes, being less labile, underwent further substitution at Ru^{III} and disproportionation at Ru^{IV}

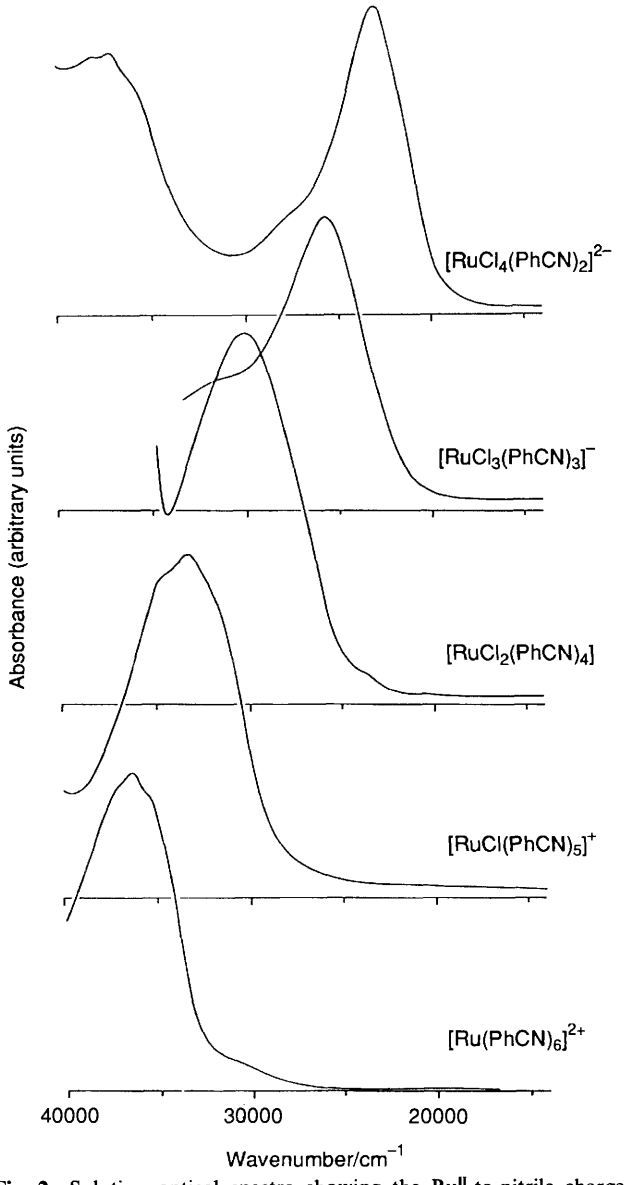

Fig. 2 Solution optical spectra showing the Ru^{II}-to-nitrile charge-transfer manifold for the series $[RuCl_{6-n}(PhCN)_n]^{4-n}$. All spectra, except that of $[RuCl_3(PhCN)_3]^-$, were collected in CH_2Cl_2 solutions, 0.5 mol dm^{-3} NBu_4BF_4 and *ca.* 10^{-3} mol dm^{-3} in sample, at low temperature (−50 to −70 °C). The spectrum for $[RuCl_3(PhCN)_3]^-$ was collected in a 5% PhCN–CH_2Cl_2 solution, 0.5 mol dm^{-3} NBu_4BF_4 and *ca.* 10^{-3} mol dm^{-3} in sample, at −30 °C

on warming. The disproportionation reaction resulted in two products: $[RuX_6]^{2-}$ and $[RuX_4(RCN)_2]^-$ [equation (1)]. The

$$2[Ru^{IV}Cl_5(RCN)]^- \longrightarrow \{Ru^{IV}Cl_4(RCN)_2\} + [Ru^{IV}Cl_6]^{2-} \quad (1)$$

$$\{Ru^{IV}Cl_4(RCN)_2\} \longrightarrow [Ru^{III}Cl_4(RCN)_2]^-$$

$$[NBu_4]_2[Ru^{IV}Cl_6] + RCN \longrightarrow [NBu_4][Ru^{III}Cl_4(RCN)_2] \quad (2)$$

progression of this reaction is not established, however it seems likely that spontaneous reduction to Ru^{III} follows halide displacement. This is also observed in the chemical synthesis of the dinitrile complex [equation (2)]. Thus, electrosynthesis is the only practicable route to the ruthenium pentahalide nitrile complexes, and the earlier claim [12] should be discounted.

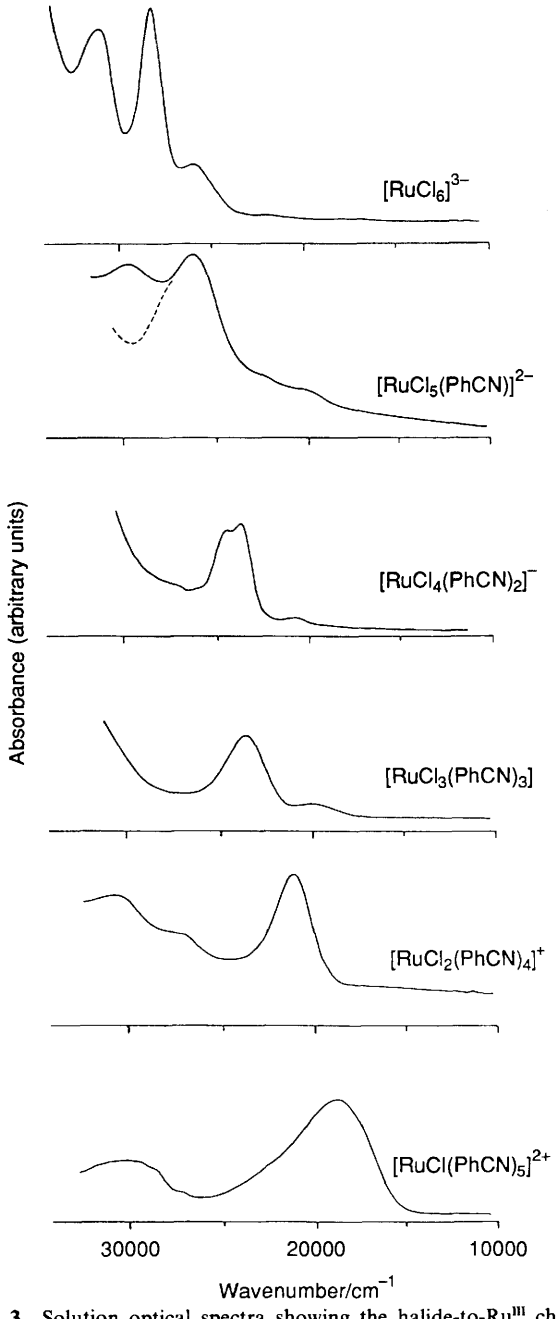

Fig. 3 Solution optical spectra showing the halide-to-Ru^{III} charge-transfer manifold for the series $[RuCl_{6-n}(PhCN)_n]^{3-n}$. All spectra, except those of $[RuCl_5(PhCN)]^{2-}$ and $[RuCl_3(PhCN)_3]$, were collected in CH_2Cl_2 solutions, 0.5 mol dm^{-3} in NBu_4BF_4 and *ca.* 10^{-3} mol dm^{-3} in sample, at low temperature (−50 to −70 °C). The spectra for $[RuCl_5(PhCN)]^{2-}$ and $[RuCl_3(PhCN)_3]$ were collected in 10 and 5% PhCN–CH_2Cl_2 solutions, 0.5 mol dm^{-3} NBu_4BF_4 and *ca.* 10^{-3} mol dm^{-3} in sample, at −50 and −30 °C, respectively

In this work the electrochemically derived products were verified by independent bench synthesis of the same complexes where possible. Those which were not prepared by chemical methods in any oxidation state are $[RuX_5(RCN)]$ and $[RuBr_3(PhCN)_3]$. The clean generation of these complexes in bulk electrolysis was substantiated by: (*i*) the appearance of single electrode potentials which are consistent with the rest of the series;[4] (*ii*) charge-transfer spectra that are consistent with other complexes of the same stoichiometry; and (*iii*) maintenance of isosbestic points during spectroelectrogeneration following the electrosynthesis. Additional support is found in comparison of the four pentahalide complexes $[RuBr_5(PhCN)]^-$, $[RuBr_5(MeCN)]^-$, $[RuCl_5(PhCN)]^-$ and $[RuCl_5$-

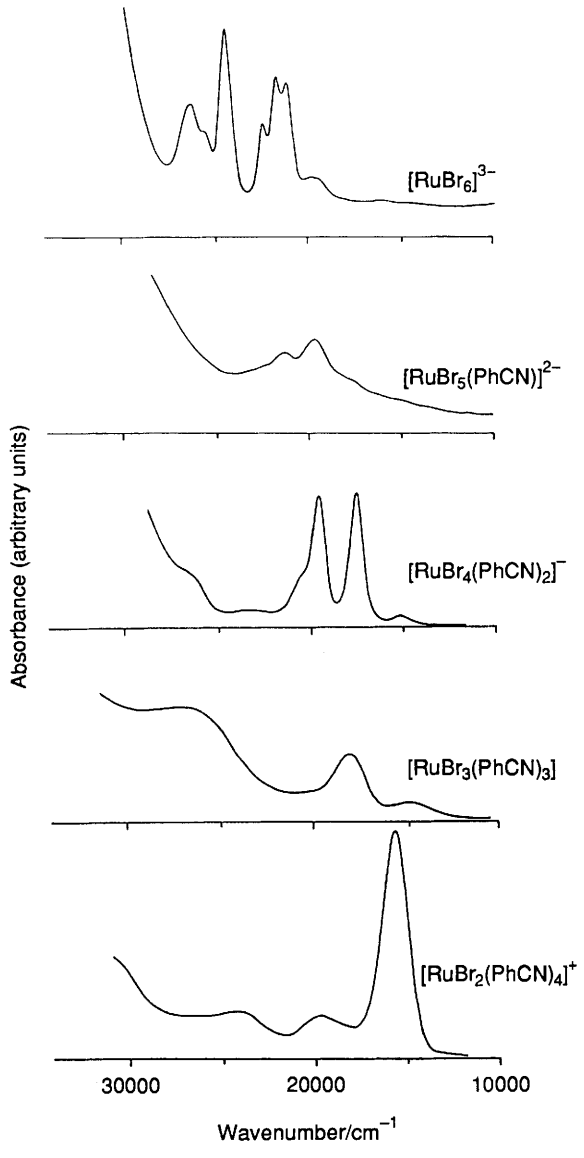

Fig. 4 Solution optical spectra showing the halide-to-Ru^{III} charge-transfer manifold for the series $[RuBr_{6-n}(PhCN)_n]^{3-n}$. All spectra, except those of $[RuBr_5(PhCN)]^{2-}$ and $[RuBr_3(PhCN)_3]$, were collected in CH_2Cl_2 solutions, 0.5 mol dm^{-3} in NBu_4BF_4 and *ca.* 10^{-3} mol dm^{-3} in sample, at low temperature (−50 to −70 °C). The spectra for $[RuBr_5(PhCN)]^{2-}$ and $[RuBr_3(PhCN)_3]$ were collected in 10% $PhCN–CH_2Cl_2$ solutions, 0.5 mol dm^{-3} NBu_4BF_4 and *ca.* 10^{-3} mol dm^{-3} in sample, at −50 °C

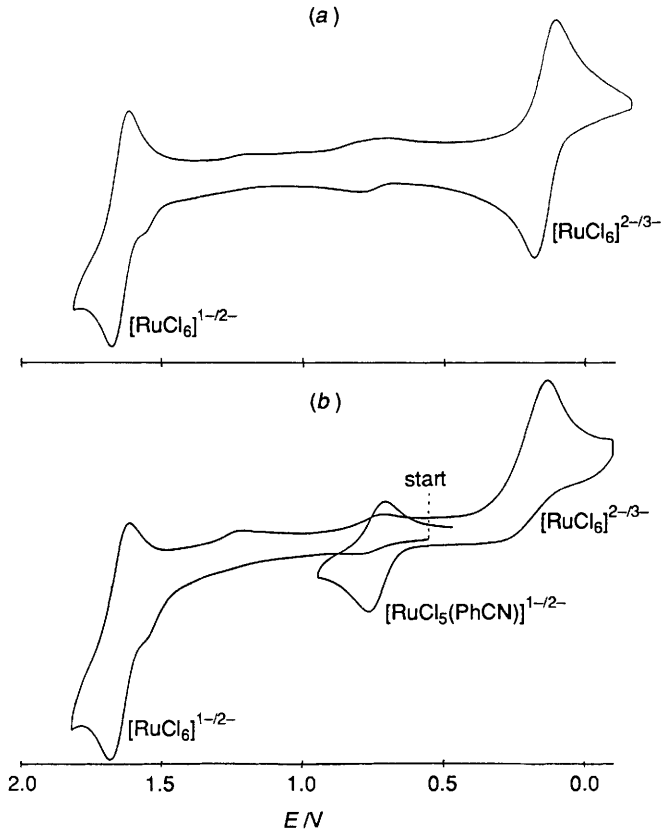

Fig. 5 Cyclic voltammograms for $[NBu_4]_2[RuCl_6]$ in 5% $MeCN–CH_2Cl_2$, 0.5 mol dm^{-3} in NBu_4BF_4 and *ca.* 10^{-3} mol dm^{-3} in sample, run at 100 mV s^{-1} in the range 0.0–2.0 V. (*a*) −60 °C, $E_{\frac{1}{2}}(Ru^{V}–Ru^{IV})$ = +1.78 V, $E_{\frac{1}{2}}(Ru^{IV}–Ru^{III})$ = 0.22 V; (*b*) ambient temperature, $E_{\frac{1}{2}}(Ru^{V}–Ru^{IV})$ = 1.78 V, cathodic peak of $[RuCl_6]^{2-}$ at 0.20 V, $E_{\frac{1}{2}}(Ru^{IV}–Ru^{III})$ of daughter product $[RuCl_5(MeCN)]$ = 0.82 V

(MeCN)]$^-$, which are self consistent in electrode potentials and charge-transfer spectra in both ruthenium-(IV) and -(III) states.

These voltammetric studies reveal that the metal-based electrode potentials are a linear function of stoichiometry when halide is progressively replaced by MeCN or PhCN. The stepwise shifts in potential are consistently 0.45 V for $Ru^{V}–Ru^{IV}$ and 0.6 V for $Ru^{IV}–Ru^{III}$ and $Ru^{III}–Ru^{II}$ for both the chloride and bromide series. These data imply a strict additivity in the co-operative influence of halide and nitrile ligands on the relevant ruthenium couples and the implications of this are discussed in detail elsewhere.[4]

Charge-transfer Spectra.—Charge-transfer spectra of complexes in multiple oxidation states were collected by electrogeneration within the spectrometer, as described above. The time-scale of an *in situ* electrolysis (minutes or hours) is much longer than a voltammetric measurement (seconds) and a reversible voltammetric response does not necessarily translate into a chemically reversible electrolysis. Loss of isosbestic points in consecutive spectra during electrolysis indicated decomposition to secondary products for the following attempted oxidations: $[RuCl_3(PhCN)_3]$ ($Ru^{IV}–Ru^{III}$), $[RuBr_4(PhCN)_2]^-$ ($Ru^{IV}–Ru^{III}$) and $[RuBr(PhCN)_5]^+$ ($Ru^{III}–Ru^{II}$), and the resultant spectra are not included in Table 3.

The irreversible electrolysis of several of the bromide complexes contrasts with that of their chloride analogues. For example, although $[RuCl_4(PhCN)_2]^-$ was reversibly oxidized to Ru^{IV} at −65 °C and +1.5 V, under the same conditions the oxidation of $[RuBr_4(PhCN)]^-$ was completely irreversible. Similarly, the oxidation of $[RuCl(PhCN)_5]^+$ at 60 °C and +1.6 V was achieved, while that of $[RuBr(PhCN)_5]^+$ failed. The most positive potential at which any of the bromide compounds were stable was +1.0 V {the oxidation of $[RuBr_2(PhCN)_4]$ at −65 °C}. These potentials are close to that required for the oxidation of free Br^- and suggest that the more labile bromide ligands dissociate to a small extent in the parent complexes.

The complex $[RuCl_3(PhCN)_3]$ is prone to condensation, forming $[Ru_2Cl_6(PhCN)_4]$ in non-co-ordinating solvents.[13] In order to prevent dimerization all experiments involving this compound were performed in the presence of *ca.* 15% benzonitrile, which limits the lowest attainable temperature within the electrolytic cell. Even under these circumstances $[RuCl_3(PhCN)_3]$ could not be oxidized reversibly so the analogous acetonitrile complex was studied, and the reversible oxidation to $[RuCl_3(MeCN)_3]^+$ was achieved in neat acetonitrile at −40 °C.

Halide to Metal Charge-transfer Spectra (*h.m.c.t.*).—The progressively substituted ruthenium(III) complexes described

Table 4 The ground state and X→M charge-transfer excited states in d_π^5 MX_x chromophores (x = 6 to 1), viewed as a progression*

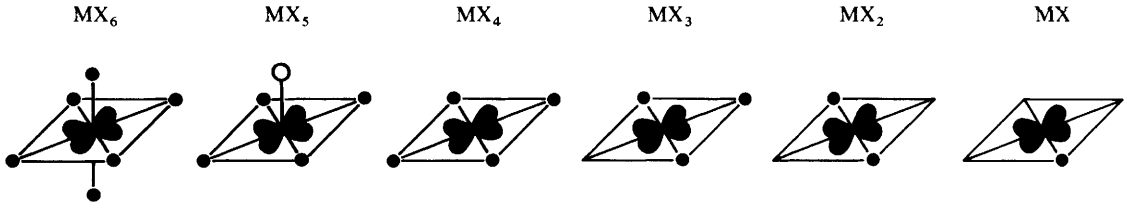

	MX_6	MX_5	MX_4	MX_3	MX_2	MX
$(d_\pi)^5$ ground state	T_{2g}	B_2	B_{2g}	B_1	E_g	E
$(d_\pi)^6(X\ \pi^*)$ c.t. states	(T_{1g})	(A_2)	(A_{2g})	B_1	—	—
	T_{1u}, T_{2u}	E	E_u	A_1	E_u	E
	(T_{2g})	B_2	B_{2g}	B_1	—	—
$(d_\pi)^6(X\ \sigma^*)$ c.t. state	T_{1u}‡	E‡	E_u‡	A_1‡	A_{2u}†	A_1†

* Only in-plane X π and X σ symmetry orbitals are considered (see text). Excited-state terms correspond directly with the symmetry of the halide-based symmetry orbital (see Fig. 6), and are listed downwards in order of increasing charge-transfer excitation energy (*i.e.* greater donor-orbital stabilization). The dominant absorption in each case is doubly underlined. Transitions to bracketed states are formally forbidden. For MX_4L_2, other authors prefer alternative assignments to spinor components of B_{2u} and A_{2u}.[16] However these transitions are non-coplanar, and electric dipole forbidden in the absence of strong ligand-based spin–orbit coupling. Their importance should increase in the corresponding iodides. † Indicates gives rise to, and ‡ free from, X_σ–X_π mixing. The z axis is always vertical, the x axis always forward.

here offer an excellent opportunity to survey the characteristic appearance and position of the optical charge-transfer manifold as a function of stoichiometry and structure. Such systematic comparisons, ranging stepwise from MX_6, through MX_n, to MX chromophores, do not seem to have been widely attempted or discussed previously. Our objective is to account for the charge-transfer spectra of the individual complexes and their relationship to one another, in a way that is clear and informative for descriptive co-ordination chemistry.

For the hexahalogenometalates the charge-transfer spectra are well understood.[14,15] Their value lies partly in the success of a straightforward unit-charge promotion model for the excited state [equation (3)]. Low-spin d^5 systems are particularly

$$[M^z(X_6{}^{6-})] \xrightarrow{h\nu} *[M^{z-1}(X_6{}^{5-})] \qquad (3)$$

instructive because electron promotion yields the closed-shell configuration (d^6, $S = 0$, $L = 0$) for the central ion. The observed spectral manifold then directly maps both the energy and the complexity of the halide symmetry orbitals. For this reason, despite its structural simplicity, $[RuCl_6]^{3-}$ is characterized by three Cl(π) to t_{2g} absorption bands (Fig. 3). These arise by promotion from the three uppermost electronic levels of the six-halide array, t_{1g}, t_{1u} and t_{2u}.

Fig. 3 shows the characteristic variation in $Cl\rightarrow Ru^{III}(t_{2g}{}^5)$ charge-transfer spectra across the series. Substitution leads to immediate simplification of the intense orbitally allowed features of $[RuCl_6]^{3-}$. The presence of a single allowed band for *trans*-$RuCl_4$, *trans*-$RuCl_2$ and RuCl chromophores is predictable, however the pentachloro complex is also dominated by one strong, though asymmetric, absorption. The additional band evident for the benzonitrile complex is due to an internal PhCN transition. Even *mer*-$[RuCl_3(RCN)_3]$ has just one principal absorption, though this is flanked by a much weaker band on either side. In contrast, conventional electric dipole selection rules would suggest *four* fully allowed transitions in both the $RuCl_5$ and $RuCl_3$ chromophores.

Our analysis of the present observations, and of scattered but congruent spectra from other sources, is based on the following simple propositions: (1) in general, transitions involving ligand-donor orbitals coplanar with the metal acceptor orbital have most intensity, *i.e.* in-plane charge-transfer transitions generally dominate the spectrum; (2) for each structure, the d-orbital vacancy is specifically located and is in the plane containing the maximum number of halide ligands, in accord with the angular overlap model.

Throughout this discussion of ruthenium(III) complexes the labels for ground and excited states correspond directly with the symmetry of the singly occupied orbital. For example, in the O_h case we can speak interchangeably of promotion from t_{1u}(Cl π) to $t_{2g}(d_\pi)$, *i.e.* $(t_{1u})^6(t_{2g})^5 \longrightarrow (t_{1u})^5(t_{2g})^6$, or of the $^2T_{2g} \longrightarrow {}^2T_{1u}$ transition, and refer for brevity to the 'T_{1u} absorption band'.

Table 4 traces the stepwise transformation of the in-plane charge-transfer transitions which accompany progressive removal of halide ligands from the parent MX_6 chromophore. It is instructive to begin by examining the ultraviolet–visible spectrum of *trans*-$[RuCl_4(PhCN)_2]^-$. This illustrates the underlying optical considerations, and also provides a good basis for explaining the spectra of neighbouring members of the series.

$[RuCl_4L_2]^-$. As shown in Table 4 and Fig. 6, the four halide ligands provide filled symmetry orbitals a_{2g}, e_u and b_{2g}, which lie in the MCl_4 plane. It can be seen that these symmetry orbitals have direct physical counterparts, t_{1g}, t_{1u}/t_{2u}, t_{2g} and $t_{1u}(\sigma)$, among the octahedral donor levels.[14] The ground state is $^2B_{2g}$, corresponding to single occupancy of the metal d_{xy} orbital. The in-plane e_u (Cl π) to b_{2g} (Ru d_π) electron transfer is the only fully allowed transition, and the favourable disposition of the e_u orbitals is clear from Fig. 6. The in-plane, but parity-forbidden, a_{2g} to b_{2g} promotion is clearly evident at lower energy and corresponds to the weak T_{1g} band of $[RuCl_6]^{3-}$. The very weak but genuine band lying a similar distance beyond the principal band is correspondingly assigned to b_{2g} to $b_{2g}(d_\pi)$ promotion. This is reinforced by the observation of a similar band for several related systems. The principal excited state ^2E_u, being orbitally degenerate, is observably split by halide-centred spin–orbit coupling. This assignment is clearly confirmed by the appropriately increased splitting observed for the tetrabromides (Fig. 4). The free-ion coefficients are 650 (Cl^-) and 2200 cm^{-1} (Br^-). The chloride σ-bonding pairs provide a further e_u donor level about 1 eV (*ca.* 1.60×10^{-19} J) lower with a corresponding well resolved absorption band at 33 000 cm^{-1}. Some mixing of the two E_u transitions is possible, as with the octahedral T_{1u} (σ, π) states. This specific assignment of the principal band has not been properly recognized before, although it is applicable to many familiar d_π^5 MX_4L_2 systems,[17–19] such as $[IrCl_4$-

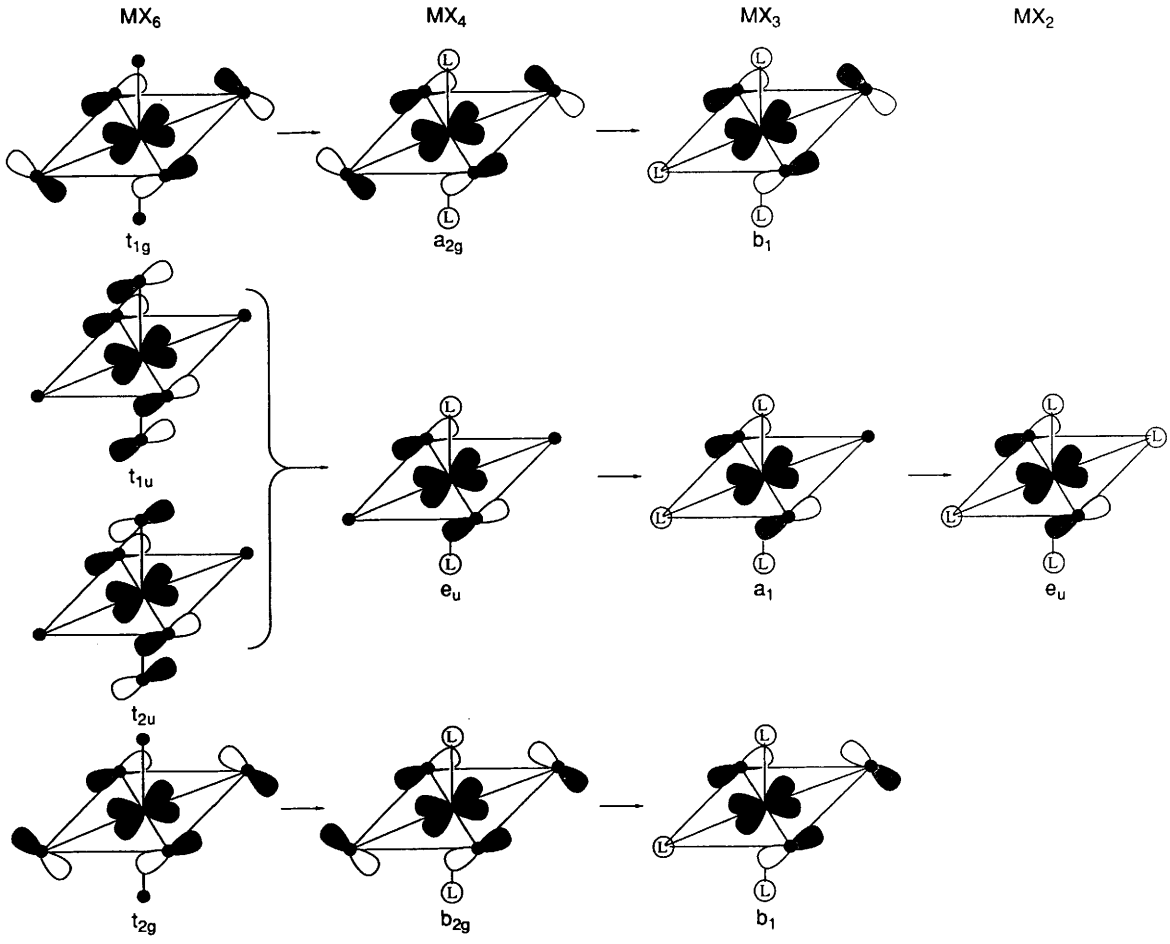

Fig. 6 Descent in complexity of halide symmetry orbitals participating in coplanar X→M optical charge transfer. Dark circles (●) locate the halide ligands in the chromophores MX_6, MX_4L_2, MX_3L_3 and MX_2L_4, while the 'four-leaf clover' shows the disposition of the unphased metal acceptor orbital. Note that in MX_6, t_{1u} and t_{2u} differ only in the phase of components which are out of the plane of the designated acceptor orbital, and this distinction vanishes in MX_4L_2. Only representative t- and e-type orbitals are shown. In MX_4L_2 the two e_u symmetry orbitals lie in the same plane and involve alternative pairs of halide ligands. In MX_2L_4 (and similarly in MXL_5) the second e orbital and the corresponding d_π acceptor orbital are obtained by 90° rotation about the M–X axis

$(PR_3)_2]$[17] and $[OsX_4(CO)(py)]^-$ (py = pyridine)[18] which show a clear-cut spectral resemblance.

$[RuCl_5(RCN)]^{2-}$. For the pentahalide chromophore the spectrum departs sharply from that of $[RuCl_6]^{3-}$. The main component of the chromophore is the equatorial $RuCl_4$ plane. For this reason the MX_5 spectra converge with those of the neighbouring *trans*-MX_4L_2 systems, and are readily assigned according to Table 4. The charge-transfer contribution from the unique apical halide is either superimposed on the main band or unobservably weak through its out-of-plane character. This pattern of one strong absorption flanked by weaker bands or shoulders has been recorded without interpretation in the scattered reports of other MCl_5L (M = Ru, Os or Ir) complexes. Spin–orbit splitting of the principal band (E) is sometimes evident, as for example for $[IrCl_5L]^-$, where L = PR_3 or SR_2.[20]

$[RuCl_3(RCN)_3]$. These complexes provide exemplary C_{2v} MX_3 chromophores. The complexes $[RuX_3(H_2O)_3]$ and $[OsX_3(H_2O)_3]$ are among the few comparable reported systems and they show very similar spectra, characterized by a major band flanked by weak shoulders. In contrast, red $[RuX_3(NH_3)_3]$ is facial, with two principal bands, and the spectra of other known *mer* compounds (L = PR_3, AsR_3, py or SR_2) are very strongly modified by L σ–X π mixing.[16] This complication is precluded by the choice of nitrile ligands.

Removal of one halide from the MX_4 *xy* plane destroys the centre of symmetry but *mer*-$[RuX_3(RCN)_3]$ retains a $(d_{xy})^1$ configuration and $^2B_2$ ground state, keeping *z* along the L–Ru–L axis (Table 4 and Fig. 6). The principal charge-transfer band, $^2B_2 \longrightarrow {}^2A_1$, is due to promotion from the symmetry orbital embracing the in-plane in-phase combination of the remaining pair of *trans* halides, now a_1, physically analogous to $e_u(x)$ in MX_4L_2. However, in the C_{2v} environment the previously parity-forbidden promotions (a_{2g} to b_{2g} and b_{2g} to b_{2g} in D_{4h}) gain further intensity as allowed in-plane transitions still straddling the principal band. Thus, in accord with Table 4, it is clear that the charge-transfer manifolds of the present *mer*-MX_3L_3 and *trans*-MX_4L_2 systems are closely related.

$[RuCl_2(RCN)_4]^+$ *and* $[RuCl(RCN)_5]^{2+}$. The ground state of *trans*-$[RuX_2(RCN)_4]^+$ is doubly degenerate, ^2E_g (d_{xy}, d_{xz}).[1] This provides a simple chromophore with one strong charge-transfer band corresponding to the one allowed transition ($E_g \longrightarrow E_u$ in D_{4h}). The monohalide system is obviously equally simple, with just one strong X π to d_π band corresponding to the $^2E \longrightarrow {}^2E$ transition. Vanquickenborne and Verdonck[21] have already analysed the h.m.c.t. behaviour of $MX(NH_3)_5$ and $MX_2(NH_3)_4$ systems in terms equivalent to the MXL_5 and MX_2L_4 assignments in Table 4.

$[RuBr_{6-n}(RCN)_n]$. Two features immediately distinguish the spectra of the chloride and bromide series: the increased complexity of the spectra for the high-symmetry bromo complexes which is due to the splitting of orbitally degenerate bands by increased ligand-based spin–orbit coupling, and the systematic energy difference between corresponding chloride and bromide bands (5600–5800 cm^{-1}), in accord with their difference in optical electronegativity. Tabulated optical electronegativity values are $X_{opt}(Cl^-) = 3.0$ and $X_{opt}(Br^-) = 2.8$, leading to an expected shift of 6000 cm^{-1} (30 ΔX_{opt}).[14,15]

The spectral complexity of $[RuBr_6]^{3-}$ compared to $[RuCl_6]^{3-}$ arises first through bromide-centred spin–orbit splitting of the T_{2u} excited state, giving Γ_7 and Γ_8 terms about 2000 cm^{-1} apart;[15] T_{1u} is also split into Γ_8 and Γ_6 but excitation to the higher component is forbidden. Likewise T_{1g} splits into $\Gamma_8(g)$ and $\Gamma_6(g)$; the lower component remains as the observed low-energy parity-forbidden band and the upper component is superimposed on the blue edge of T_{1u} (Γ_8). The additional fine structure on each band is due to characteristic Jahn–Teller splitting in the heavier hexahalide. The charge-transfer spectra of all such d^5 hexabromides are very similar in appearance.[15]

The spectra of the MBr_5 through MBr_2 systems are similar to those of their chloride analogues. The marked increase in spin–orbit splitting of the doublet transitions, $E(RuBr_5)$ and $E_u(RuBr_4)$, reinforces the listed assignments. For MX_3 the charge-transfer excited states are orbitally non-degenerate so that ligand-based spin–orbit coupling is not operative, and the chloride and bromide spectra are essentially superimposable. The observation of a single charge-transfer band for *trans*-$[RuBr_2(RCN)_4]^+$ can be explained since detailed analysis shows that only one of the two expected spin–orbit components of the $E_u(MX_2)$ transition [$\Gamma_6(u)$] gains intensity by polarization along the X–M–X axis.

The corresponding halide-to-ruthenium(IV) charge-transfer manifolds are systematically shifted by 6000 cm^{-1} to lower energy and of generally similar appearance to those of their ruthenium(III) analogues (Table 3 and Fig. 1).

Metal-to-Ligand Charge-transfer Spectra (*m.l.c.t.*).—In other contexts the analysis of Ru^{II}-to-ligand optical charge-transfer spectra has aroused enormous attention.[22] Our data offer an unrivalled opportunity for studying a set of simple m.l.c.t. chromophores varying from *trans*-ML_2 to ML_6. As illustrated in Fig. 2, a single m.l.c.t. band is found for each complex in the series $[RuX_{6-n}(PhCN)_n]^{n-4}$, despite the wide variation in molecular structure and formal symmetry. The band moves steadily to higher frequencies with increasing number of nitrile ligands, and replacement of chloride by bromide has little effect on the appearance or position of the absorption band. The analysis corresponds closely in formal symmetry terms with our previous description of h.m.c.t. chromophores, since each nitrile ligand contributes two mutually perpendicular π^* acceptor orbitals. However, m.l.c.t. promotion from the ruthenium(II) d_π^6 ground state may involve any of the three d orbitals, in contrast to h.m.c.t. processes where the hole in the ruthenium(III) d shell is specifically located.

$[RuX_5(PhCN)]^{3-}$ *and* $[RuX_4(PhCN)_2]^{2-}$. In *trans*-$[RuX_4(RCN)_2]^{2-}$ promotion from $e_g(d_{xz}, d_{yz})$ to $e_u(L\ \pi^*\ x, y)$ is spatially favoured and *z* polarized, where *z* defines the unique axis bearing the two nitrile ligands. Promotion from d_{xy} to L π^* is formally allowed but disqualified through being out of plane. Similarly, there should be one intense absorption for the inaccessible $[RuCl_5(RCN)]^{3-}$, arising from d_{xz} and d_{xy} to e(L π^*) electron transfer and located at 19 700 cm^{-1} (by extrapolation).

Zwickel and Creutz analysed the m.l.c.t. spectra of divalent $[Ru(NH_3)_5(py)]^{2+}$ and *trans*-$[Ru(NH_3)_4(py)_2]^{2+}$ similarly, and showed that each complex should be characterized by a single parity-allowed $Ru^{II}\rightarrow$py charge-transfer absorption. Unlike nitrile, each pyridine ligand contributes only one appropriate π^* acceptor orbital to the chromophore, but the reasoning is the same in both studies.

$[RuX_2(PhCN)_4]$. Turning to *trans*-$[RuX_2(PhCN)_4]$ and locating *z* orthogonal to the equatorial plane, we note the ligand-orbital arrangements are exactly as in the *trans*-MX_4 chromophore. The eight π^* orbitals (one vertical and one equatorial from each nitrile ligand) generate the symmetry orbitals a_{2u}, e_u, b_{2u}, and b_{2g}, e_g, a_{2g}. Only the u levels are relevant for parity-allowed transitions, and of these e_u lies in the *xy* plane whereas a_{2u} and b_{2u} are built of vertical components. We then predict three spatially favoured transitions, which are all *xy* polarized, as shown. The ligand–ligand covalent interactions which separate the acceptor levels seem likely to be energetically small, as borne out by the simplicity of the hexakis(nitrile) l.m.c.t. spectrum (see below).

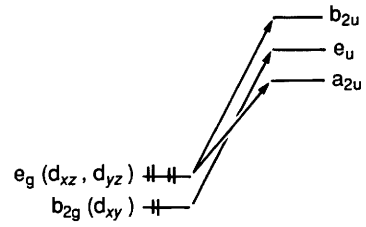

$[Ru(PhCN)_6]^{2+}$. Naturally, in the O_h case there is no distinction between promotions from the d_{xz}, d_{yz} or the d_{xy} orbitals, and so the analyses of ML_6 m.l.c.t. and MX_6 h.m.c.t. are formally equivalent. Thus $[Ru(PhCN)_6]^{2+}$ should have parity-allowed transitions to the nitrile L $\pi^*(t_{1u})$ and L $\pi^*(t_{2u})$ symmetry orbitals. Just one well defined band is observed. Therefore either the t_{1u} and t_{2u} promotions are close in energy and not resolved, or improbably the t_{2u} transition lies at higher energy and out of sight. In the hexachlorides the $t_{1u} - t_{2u}$ separation is 3000 cm^{-1}, having been strongly modified by mixing with the first σ t_{1u} level. Such complications should not arise in $[Ru(PhCN)_6]^{2+}$ since the corresponding PhCN σ orbitals are energetically remote from PhCN $\pi^*(t_{1u})$.

$[RuX(PhCN)_5]^+$ *and* $[RuX_3(PhCN)_3]^-$. Approaching $[RuX(PhCN)_5]^+$ from $[RuX_2(PhCN)_4]$, in addition to retaining the equatorial transitions, a new band might be expected due to efficient $e(d_{xz}, d_{yz})$ to e(PhCN axial) promotion, but just one major band is observed. Similarly, only one absorption band and a high-energy shoulder is observed for $[RuX_3(PhCN)_3]^-$. Evidently, in these low-symmetry systems, neither ligand-field splitting of the occupied d_π orbitals nor molecular-orbital differentiation of the nitrile acceptor levels is sufficient to separate the expected transitions, though there is some evidence of unresolved components.

In summary, these observations offer a coherent summary of what may be expected in both h.m.c.t. (Ru^{III}) and m.l.c.t. (Ru^{II}) spectra in an exhaustive substitution series where the nitrile ligand is itself optically transparent, redox-inert and not subject to σ–π mixing as is the case with S and P donor ligands. The h.m.c.t. (Ru^{III}) transitions show a marked and steady descent in energy through the chromophoric sequence MX_6, MX_5, MX_4 and likewise in the sequence MX_3, MX_2, MX, although the band is essentially stationary between MX_4 and MX_3 (overall, -1930 cm^{-1} per Cl^- lost; -1800 cm^{-1} per Br^- lost). The general trend is apparent in Figs. 3 and 4, and is readily associated with the characteristically strong shift in $E_{\frac{1}{2}}(Ru^{III}–Ru^{II})$ for the same complexes (*ca.* 0.6 V per halide lost). In other words, the overall red shift of the charge-transfer manifold between $[RuX_6]^{3-}$ and $[RuX(RCN)_5]^{2+}$ is a natural reflection of the increasing ease of reduction of the central ion. Taken in isolation, Taube's[24] pioneering study on $[OsCl_{6-n}(NH_3)_n]^{n-3}$ complexes could suggest that the h.m.c.t. transition energies are little affected by progressive substitution. However, the present work demonstrates that in the very many instances where the substituting ligand significantly stabilizes the metal d_π orbitals (nitriles, phosphines, pyridine, *etc.*) there will be a rational trend to lower frequencies in the $MX_{6-n}L_n$ h.m.c.t. manifold. The clear-cut and uniform trend in the m.l.c.t. spectra is actually steeper, and opposite in sign to the complementary trends in the h.m.c.t. spectra (*ca.* 3300 cm^{-1} per halide lost).

Elsewhere we have used these data to construct a conceptual representation of the progressive changes in the relative frontier-orbital energies of ruthenium, halide, and nitrile ligands throughout the series.[4]

References

1 V. T. Coombe, G. A. Heath, T. A. Stephenson, J. D. Whitelock and L. J. Yellowlees, *J. Chem. Soc., Dalton Trans.*, 1985, 947.
2 K. J. Taylor and L. J. Yellowlees, XXVII International Conference on Coordination Chemistry, Broadbeach, Australia, 1989, abstract W35.
3 S. Brownstein, G. A. Heath, A. Sengupta and D. W. A. Sharp, *J. Chem. Soc., Chem. Commun.*, 1983, 669; G. A. Heath, K. A. Moock, D. W. A. Sharp and L. J. Yellowlees, *J. Chem. Soc., Chem. Commun.*, 1985, 15.
4 C. M. Duff and G. A. Heath, *Inorg. Chem.*, 1991, **30**, 2528.
5 E. A. Seddon and K. R. Seddon, *The Chemistry of Ruthenium*, Elsevier, New York, 1984, p. 162.
6 W. Preetz and N. H. Allworden, *Z. Naturforsch., Teil B*, 1987, **42**, 381.
7 J. E. Fergusson and A. M. Greenaway, *Aust. J. Chem.*, 1978, **31**, 497.
8 J. Dehand and J. Rose, *J. Chem. Res.*, 1979, (*M*) 2167.
9 W. Luginbuhl, A. Ludi, A. Raselli and H. B. Burgi, *Acta Crystallogr., Sect. C*, 1989, **45**, 1428.
10 P. Bernhard, Doctoral Thesis, Universitat Bern, 1984.
11 C. Duff, G. A. Heath and A. C. Willis, *Acta Crystallogr., Sect. C*, 1990, **46**, 2320.
12 J. Dehand and J. Rose, *Inorg. Chim. Acta*, 1979, **37**, 249.
13 C. M. Duff, G. A. Heath and T. J. Khoo, unpublished work.
14 C. K. Jorgenson, *Mol. Phys.*, 1959, **2**, 309.
15 C. K. Jorgenson, *Prog. Inorg. Chem.*, 1970, **12**, 101.
16 A. J. McCaffrey and M. D. Rowe, *J. Chem. Soc., Faraday Trans. 2*, 1973, 1767.
17 M. D. Rowe, A. J. McCaffrey, R. Gale and D. N. Copsey, *Inorg. Chem.*, 1972, **11**, 3090.
18 K. G. Greulich and W. Preetz, *J. Organomet. Chem.*, 1981, **220**, 201.
19 R. A. Cipriano, W. Levason, R. A. S. Mould, D. Pletcher and M. Webster, *J. Chem. Soc., Dalton Trans.*, 1990, 339; R. A. Cipriano, W. Levason, D. Pletcher, N. A. Powell and M. Webster, *J. Chem. Soc., Dalton Trans.*, 1987, 1901; G. J. Leigh and D. M. P. Mingos, *J. Chem. Soc. A*, 1970, 587; T. A. Stephenson, *J. Chem. Soc. A*, 1970, 889.
20 R. A. Cipriano, W. Levason, R. A. S. Mould, D. Pletcher and N. A. Powell, *J. Chem. Soc., Dalton Trans.*, 1988, 2677.
21 L. G. Vanquickenborne and E. Verdonck, *Inorg. Chem.*, 1974, **13**, 762.
22 A. Juris, V. Balzani, F. Barigelletti, S. Campagna, P. Belser and A. von Zelewsky, *Coord. Chem. Rev.*, 1988, **84**, 85.
23 A. M. Zwickel, and C. Creutz, *Inorg. Chem.*, 1971, **10**, 2395.
24 J. D. Buhr, J. R. Winkler and H. Taube, *Inorg. Chem.*, 1980, **19**, 2416.

Received 30*th January* 1991; *Paper* 1/00439E